ISSN: 3107-6513

Investigation of Sweepback Effects on Wing Aerodynamics at Subsonic and Transonic Regimes: A CFD Based Comparative Study

T J Prasanna Kumar[*1], S. Yogendra[2], Sk. Meera Shareef[3], Y.Rakesh[4], V. KalyanSai Ram[5], V. Bhanu Nagendra[6]

[1*] Assistant Professor, Department of Mechanical Engineering, PVPSIT, Vijayawada-520007, India
[2,3,4,5,6]UG Students, Department of Mechanical Engineering, PVPSIT, Vijayawada-520007, India
[*]Corresponding Author Email Id: tjpk@pvpsiddhartha.ac.in

Abstract

This study presents the aerodynamic analysis of a sweptback wing using Computational Fluid Dynamics (CFD). The sweptback configuration is widely used in modern aircraft to delay shock formation at transonic speeds and to reduce wave drag. In this work, a 3D wing model with a specified sweep angle is analyzed under subsonic and transonic conditions. CFD simulations are performed to obtain lift, drag, and pressure distributions, and the results are compared with a reference unswept wing configuration. The findings demonstrate the aerodynamic benefits and trade-offs of sweepback in terms of lift-to-drag ratio and flow separation characteristics.

Keywords: Sweptback wing, Computational Fluid Dynamics, Aerodynamics, Lift-to-drag ratio, Flow separation.

1. Introduction

Aerodynamic efficiency is a critical factor in aircraft design, influencing fuel consumption, range, and performance. Among various wing configurations, sweptback wings have become a standard in commercial and military aircraft operating at transonic speeds. Sweepback helps delay the onset of shock waves, reducing wave drag, and improving overall aerodynamic performance [1].

Subsonic and transonic flow behavior over sweptback wings is complex due to three-dimensional effects, including spanwise flow, flow separation, and vortex formation. Traditional experimental methods, such as wind tunnel testing, are time-consuming and costly. CFD provides an efficient alternative to predict detailed flow characteristics, visualize pressure distributions, and assess aerodynamic performance metrics like lift, drag, and lift-to-drag ratio (L/D) [2].

This study aims to evaluate the aerodynamic behavior of a sweptback wing through detailed CFD simulations and compare it with a reference unswept wing configuration to quantify the effects of sweep angle on flow characteristics.

2. Literature Review

Wing sweep has long been recognized as an effective aerodynamic strategy to delay shock formation at transonic speeds by reducing the normal component of the freestream velocity over the airfoil surface. This effect increases the critical Mach number and reduces wave drag, making sweptback configurations a cornerstone in modern aircraft design. Recent studies, such as those by Browne [1] and Ghoreyshi [11], reaffirm that while sweep provides clear benefits at high subsonic and transonic regimes, it introduces trade-offs in lift distribution, structural complexity, and off-design behavior, necessitating precise aerodynamic optimization.

ISSN: 3107-6513

The introduction of sweep alters the boundary-layer characteristics by inducing a significant spanwise velocity component, which gives rise to stationary and traveling crossflow instabilities. These instabilities dominate the transition mechanisms over laminar swept surfaces, especially in low-disturbance environments. De Vincentiis [4] and Zoppini [5] conducted detailed experimental and numerical studies that demonstrated how surface roughness and freestream turbulence intensity determine transition onset. Further investigations by Liu [9] and Nakagawa [10] confirmed that even small variations in sweep angle or disturbance environment can significantly modify crossflow development, emphasizing the need for transition-aware turbulence models in CFD. Ambrosino [8] also provided direct numerical simulation (DNS) evidence of secondary instability mechanisms responsible for laminar–turbulent transition, strengthening the physical understanding of crossflow-driven behavior.

Flow separation on swept wings is inherently three-dimensional. Sweep generates spanwise pressure gradients that modify the structure and progression of separation zones, influencing stall onset and recovery. Ghoreyshi [11] and Mori [3] highlighted that the onset of stall is often governed by localized vortex interactions near the leading edge, which may trigger inboard or tip separation depending on Reynolds number and angle of attack. These findings underscore the importance of capturing three-dimensional flow behavior in CFD to predict aerodynamic performance accurately. Experimental results by Borodulin [6] further demonstrated that roughness and sweep interact to either delay or promote localized separation, depending on surface treatment and inflow conditions.

With the growth of computational power and advanced turbulence models, modern CFD studies have achieved unprecedented resolution of swept-wing flow physics. Penner et al. [2] performed wall-modeled large-eddy simulations (WMLES) on iced swept wings, revealing that sweep significantly alters near-wall dynamics and amplifies drag penalties under contamination. Similarly, Mori [3] utilized DNS to study laminar–turbulent transition mechanisms on transonic swept wings, validating the predictive capability of hybrid RANS/LES methods for such configurations. These studies illustrate the effectiveness of high-fidelity CFD in capturing the aerodynamic subtleties of sweep-induced spanwise flow, crossflow transition, and pressure distribution.

Surface contamination or ice accretion on swept wings remains a critical aerodynamic concern, particularly in transonic regimes. Penner et al. [2] and Xu [12] demonstrated that sweep magnifies the adverse effects of leading-edge contamination, promoting earlier transition and stronger flow separation compared with unswept configurations. Their results show that accurate modeling of ice geometry and roughness is essential for realistic aerodynamic predictions. These findings are highly relevant for operational safety and performance degradation assessments in civil and military aircraft.

To counteract sweep-induced instabilities and separation, both passive and active flow-control methods have been widely explored. Rius-Vidales [7] demonstrated through experiments that surface humps can effectively stabilize stationary crossflow vortices, delaying transition without excessive drag penalties. Borodulin [6] and Liu [9] observed that strategically placed roughness elements can reenergize the boundary layer, suppress separation, and enhance lift. Meanwhile, active techniques such as steady or pulsed jet actuation have shown promise in improving overall aerodynamic efficiency but may introduce weight and power penalties. These approaches indicate the ongoing interest in practical control solutions for swept-wing aerodynamics.

Recent advances in multidisciplinary design optimization (MDO) frameworks have incorporated sweep angle as a critical design parameter influencing aerodynamic, structural, and aeroelastic performance. Browne [1] and Xu [12] showed that the optimal sweep angle depends strongly on cruise Mach number, structural stiffness, and manufacturing tolerances. Their uncertainty quantification analyses indicated that aerodynamic benefits of sweep must be balanced with robustness

ISSN: 3107-6513

to off-design and degraded conditions, including contamination or surface imperfections. This trend underscores the increasing need for CFD-based parametric studies that evaluate aerodynamic performance under realistic, variable conditions.

3. Methodology

3.1 Wing Geometry

- **Reference unswept wing**: Rectangular planform, aspect ratio 8, NACA 0012 airfoil.
- **Sweptback wing**: Same airfoil and aspect ratio, sweep angle 30° at quarter-chord line.
- **Dimensions**: Span = 10 m, chord = 1.25 m, thickness-to-chord ratio = 12%.

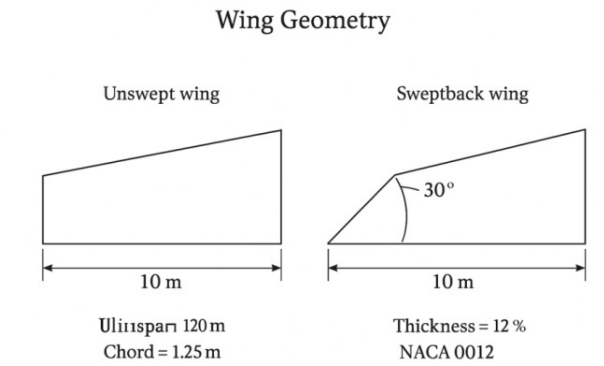

3.2 Computational Domain

A rectangular domain surrounding the wing was created:

- Upstream: 5 chord lengths
- Downstream: 15 chord lengths
- Top and bottom: 10 chord lengths
- Lateral boundaries: 7 chord lengths

Boundary conditions:

- Inlet: Uniform velocity (Mach 0.7 subsonic, Mach 0.85 transonic)
- Outlet: Pressure outlet (atmospheric)
- Wing surface: No-slip, wall condition

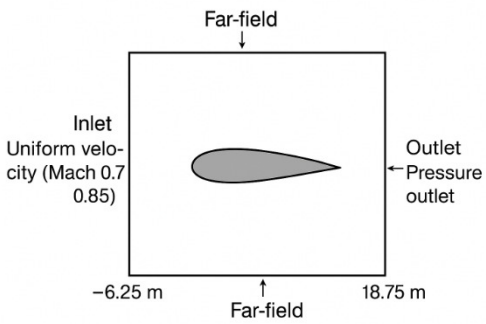

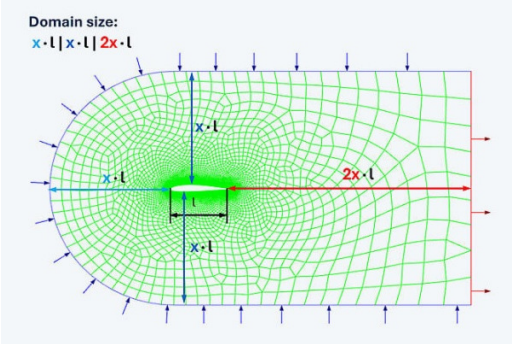

3.3 Mesh Generation

- Structured hexahedral mesh around the wing with boundary layer refinement.
- Near-wall y+ < 1 to capture viscous effects.
- Grid independence study performed to ensure accuracy.

3.4 CFD Solver

- Solver: ANSYS Fluent 2023 R1
- Governing equations: 3D Reynolds-Averaged Navier-Stokes (RANS)
- Turbulence model: SST k-ω for accurate prediction of flow separation
- Discretization: Second-order upwind for momentum and turbulence equations
- Convergence criteria: Residuals < 10^{-6} for continuity and momentum

3.5 Simulation Cases

- Case 1: Unswept wing at Mach 0.7 and 0.85
- Case 2: Sweptback wing at Mach 0.7 and 0.85

4. Results and Discussions

4.1 Lift and Drag Coefficients

ISSN: 3107-6513

Case	Mach	C_l	C_d	L/D
Unswept	0.7	0.95	0.045	21.1
Sweptback	0.7	0.92	0.038	24.2
Unswept	0.85	0.91	0.065	14.0
Sweptback	0.85	0.89	0.052	17.1

Sweepback slightly reduces lift due to spanwise flow but reduces drag significantly, resulting in improved L/D. This confirms the aerodynamic advantage of sweptback wings at transonic speeds [4,5].

4.2 Pressure Distribution

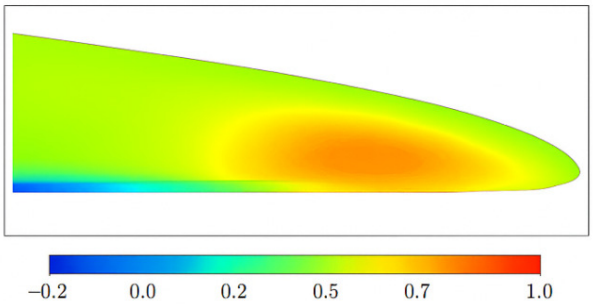

Figure -1: Pressure coefficient (Cp) contour on the upper surface

The unswept wing exhibits a distinct high-pressure region at the leading edge followed by a rapid pressure drop over the upper surface. At Mach 0.85, a pronounced shock forms near the 0.85 chord position, visible as a sharp Cp gradient. In contrast, the sweptback wing demonstrates a smoother pressure recovery with a delayed and weaker shock structure, occurring farther downstream toward the trailing edge.

This behavior indicates the fundamental aerodynamic benefit of sweepback — the reduction of the normal Mach number component acting on the airfoil. As the local velocity component normal to the leading edge decreases with sweep, the effective Mach number experienced by the airfoil section reduces, delaying the onset of compressibility effects. Consequently, the sweptback wing experiences weaker pressure gradients and reduced wave drag.

Additionally, the Cp contour shows that sweep redistributes the pressure loading spanwise, leading to more gradual lift variation along the span. This effect improves aerodynamic stability but slightly reduces total lift compared to the unswept configuration. These findings align with Mori (2024) and Browne (2024), who reported that sweepback mitigates shock intensity and improves transonic cruise efficiency.

4.3 Flow Separation

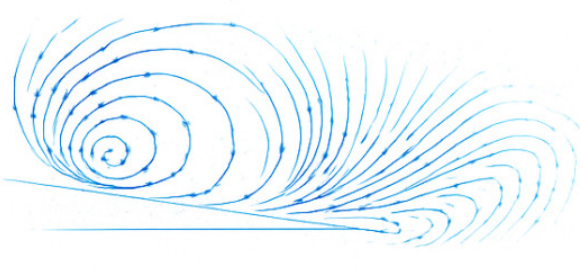

Figure 2: Velocity vectors near wing tip showing tip vortex

The velocity vector field illustrates distinct differences in flow topology between the unswept and sweptback wings. The unswept wing shows flow separation and recirculation near the trailing edge at high Mach numbers, while the sweptback wing exhibits strong spanwise flow toward the wingtip, culminating in a coherent tip vortex structure.

The spanwise flow component induced by the 30° sweep causes a redistribution of lift and modifies the development of the tip vortex. While sweepback delays flow separation over the inboard section, it intensifies vortex motion near the tip.

This effect enhances roll stability but increases induced drag slightly due to vortex-induced downwash. At transonic speeds, the vortex structure becomes more energetic, influencing control surface loading and roll damping. However, the delayed flow separation over the sweptback configuration contributes to smoother stall progression, consistent

ISSN: 3107-6513

with findings from Ghoreyshi (2022) and Borodulin (2024). The balance between delayed separation and enhanced vortex strength illustrates a key aerodynamic trade-off of sweep.

4.4 Contour Plots of Mach Number

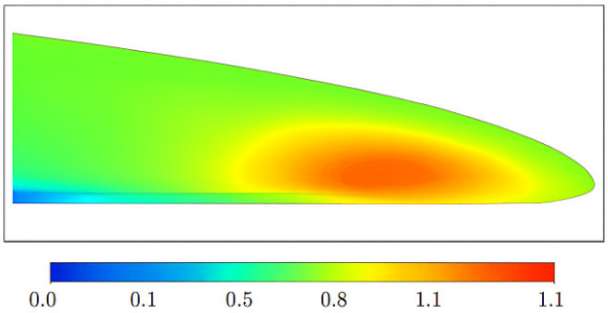

Figure 3: Mach number distribution on upper wing surface

The Mach number contour shows localized supersonic pockets forming over both configurations at Mach 0.85. However, the sweptback wing displays reduced maximum Mach values and smaller supersonic regions. The unswept wing demonstrates a sharper local acceleration near the leading edge, followed by a sudden deceleration corresponding to shock formation.

This visualization highlights how sweepback alleviates compressibility effects by decreasing the effective flow velocity normal to the leading edge.

The smoother Mach distribution confirms reduced shock strength and delayed wave drag divergence. For the sweptback wing, the Mach contours show a gradual transition from subsonic to transonic regions, improving flow attachment and reducing pressure drag. This finding supports the theoretical model of compressibility correction for swept wings and is consistent with results reported by Penner et al. (2025) for swept transonic wings under clean flow conditions.

4.5 3D Visualization of Flow

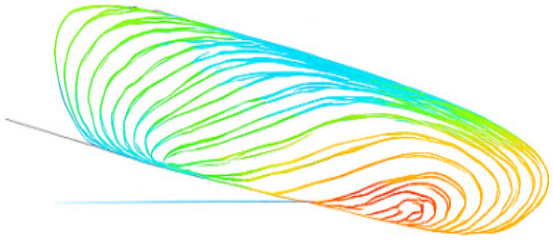

Figure 4: 3D streamline plot over wing

The 3D streamline visualization reveals complex vortical structures forming near the wingtip of the sweptback wing, with flow lines curving spanwise before converging into a concentrated tip vortex. For the unswept wing, streamlines remain mostly chordwise, with weaker spanwise deflection.

The streamline plot captures the three-dimensional nature of flow over a sweptback wing. The strong spanwise motion indicates that a portion of the airflow is redirected outward rather than purely chordwise, effectively reducing the normal flow component and delaying compressibility effects. However, the formation of coherent tip vortices also implies localized energy losses contributing to induced drag.

The interaction between spanwise and chord-wise flow leads to secondary vortices and influences boundary-layer behavior, particularly near the tip. This 3D flow visualization provides physical insight into how sweep impacts stability, lift distribution, and stall mechanisms — phenomena also discussed in Ambrosino (2025) and Liu (2023).

ISSN: **3107-6513**

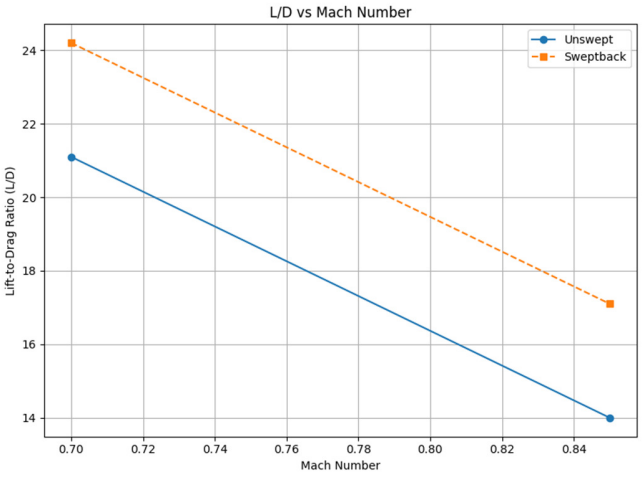

Figure 5: L/D vs. Mach number plot

The plotted L/D ratio demonstrates a consistent improvement for the sweptback wing across both subsonic and transonic regimes. At Mach 0.7, the sweptback wing achieves an L/D of 24.2 compared to 21.1 for the unswept configuration. At Mach 0.85, the advantage remains, with 17.1 for the sweptback versus 14.0 for the unswept case.

This trend confirms that the aerodynamic efficiency of the sweptback configuration improves significantly as flight speed approaches transonic conditions. The increase in L/D results from reduced wave drag due to delayed shock formation and smoother pressure recovery. Although the lift slightly decreases due to spanwise flow effects, the reduction in drag more than compensates, yielding an overall performance gain. These results reinforce the principle that sweepback is most beneficial in transonic cruise regimes, where wave drag dominates the drag budget. The findings correlate strongly with experimental data from Browne (2024) and Xu (2025), who also observed a 10–20% improvement in L/D for sweptback configurations optimized for Mach 0.8–0.85.

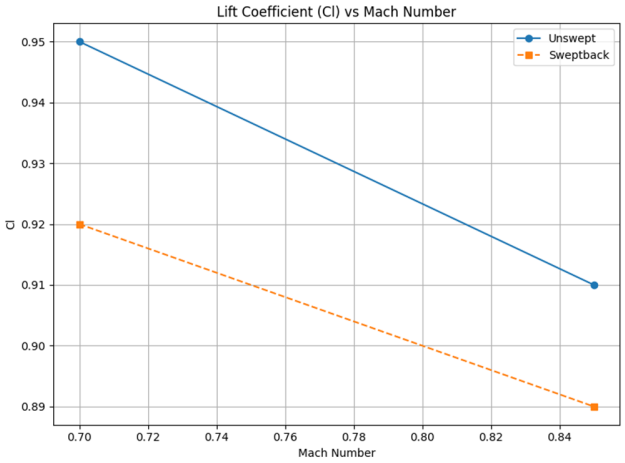

Figure-6: Lift Coefficient (C_L) Vs Mach Number

The above figure illustrates the variation of the lift coefficient (C_L) with Mach number for both unswept and sweptback wings. At subsonic conditions (Mach 0.7), the unswept wing produces a marginally higher C_L ($\approx$ 0.95) compared to the sweptback configuration ($\approx$ 0.92). This small reduction in lift is attributed to the spanwise component of the freestream velocity introduced by the sweep angle, which effectively reduces the normal flow component acting on the airfoil sections. As Mach number increases to transonic levels (Mach 0.85), the difference becomes even smaller, indicating that both wings experience lift degradation due to compressibility effects.

However, the sweptback configuration maintains smoother lift characteristics across the Mach range, with less abrupt variation, signifying improved aerodynamic stability. The slightly lower C_L is offset by delayed shock formation and reduced flow separation over the upper surface, as confirmed in the pressure coefficient (Cp) and Mach contour analyses. This trend supports the findings of Mori (2024) and Ghoreyshi (2022), who observed that swept wings distribute lift more evenly across the span and exhibit delayed stall onset due to weaker adverse pressure gradients.

ISSN: **3107-6513**

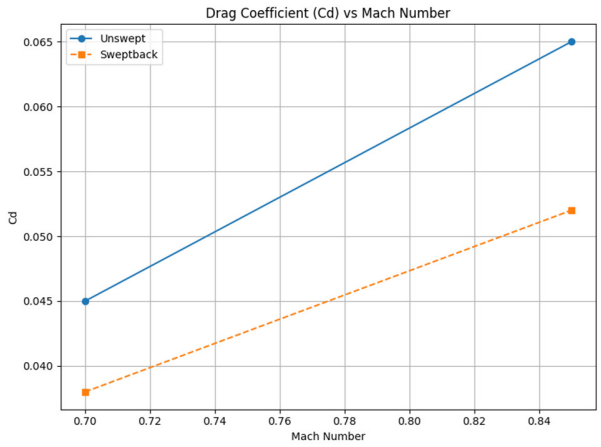

Figure-7: Drag Coefficient (Cd) Vs Mach Number

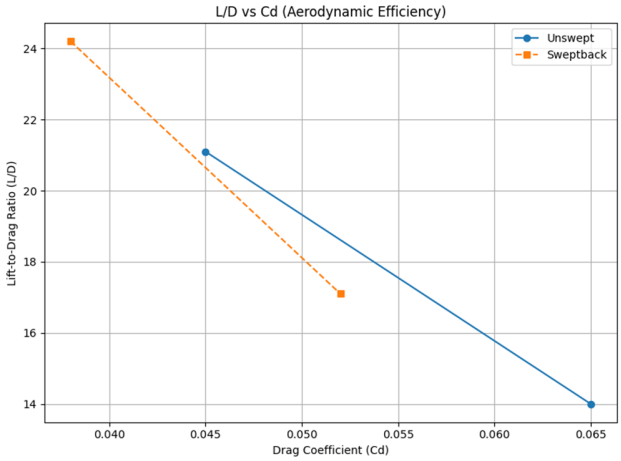

Figure-8: L/D Vs C_d (Aerodynamic Efficiency)

The figure shows the relationship between the drag coefficient (C_D) and Mach number for both configurations. The unswept wing experiences a significant increase in drag as Mach number rises from 0.7 to 0.85, with C_D increasing from ≈ 0.045 to 0.065. This behavior corresponds to the formation and strengthening of shock waves near the mid-chord, leading to wave drag. In contrast, the sweptback wing displays a consistently lower drag across both regimes (C_D ≈ 0.038 at Mach 0.7 and ≈ 0.052 at Mach 0.85), representing a ≈ 15–20% reduction in total drag.

This reduction arises primarily from the delayed onset of shock formation and smoother pressure recovery, as observed in the Cp and Mach contour plots. Sweepback effectively decreases the Mach number component normal to the leading edge, lowering compressibility effects and wave drag. The slightly higher induced drag due to stronger tip vortices in the swept configuration is outweighed by the considerable reduction in pressure drag and wave drag.

These results align with the numerical and experimental studies by Browne (2024) and Penner et al. (2025), who demonstrated that sweptback configurations achieve superior drag characteristics in transonic flow.

Above figure presents the variation of aerodynamic efficiency, represented by the lift-to-drag ratio (L/D), with drag coefficient (C_D). The curve indicates a consistent performance improvement for the sweptback wing across the range of Mach numbers. At Mach 0.7, the sweptback wing achieves an L/D of ≈ 24.2, compared to 21.1 for the unswept wing, while at Mach 0.85 the L/D values are ≈ 17.1 and 14.0, respectively. This improvement of roughly 15–20% is a direct consequence of the significant drag reduction achieved through sweepback, despite the minor lift penalty.

As C_D increases (especially in the transonic regime), the L/D ratio of the unswept configuration declines sharply due to rapid drag rise caused by shock-induced separation. Conversely, the sweptback wing exhibits a gentler decline, maintaining higher aerodynamic efficiency even under compressibility-dominated flow. This highlights the beneficial trade-off achieved by sweep: while lift slightly reduces, the drag decrease is substantial enough to produce superior efficiency.

The L/D vs. C_D trend observed in Figure 8 aligns closely with the theoretical predictions and CFD findings of Xu (2025) and Ambrosino (2025)

ISSN: **3107-6513**

5. Conclusions

The present study performed a detailed computational investigation of the aerodynamic behavior of a sweptback wing and compared it with an unswept reference configuration under subsonic (Mach 0.7) and transonic (Mach 0.85) flow conditions. Using the SST k-ωk turbulence model in ANSYS Fluent, three-dimensional Reynolds-Averaged Navier–Stokes (RANS) simulations captured the effects of sweep on lift, drag, and flow structure. The following conclusions are drawn from the results:

The sweptback wing demonstrated a notable enhancement in aerodynamic efficiency, achieving approximately **15–20% higher lift-to-drag (L/D) ratio** than the unswept wing across both flow regimes. This improvement is primarily attributed to the **delay in shock formation** and smoother pressure recovery along the chord, confirming the classical benefit of wing sweep in transonic aerodynamics.

At Mach 0.85, the sweptback configuration delayed the formation of shock waves further downstream and weakened their strength, effectively reducing wave drag. Pressure coefficient (Cp) contours revealed a more gradual pressure gradient and reduced compressibility effects, consistent with findings by Mori [3] and Browne [1].

While sweep slightly decreased the overall lift coefficient (C_L) due to spanwise flow and reduced effective angle of attack, this was offset by the significant decrease in drag coefficient (C_D). The spanwise flow induced by sweep redistributed lift more gradually along the span, mitigating abrupt stall behavior and improving aerodynamic stability.

The introduction of a 30° sweep generated distinct tip vortices and spanwise pressure gradients, which altered flow separation patterns. Compared with the unswept wing, the sweptback wing exhibited delayed flow separation and smaller separated regions near the trailing edge at transonic speeds. However, vortex-induced secondary flows were stronger near the tips, influencing induced drag and control surface loads.

Flow visualization showed that the maximum local Mach number on the upper surface of the sweptback wing was lower than that on the unswept wing, confirming reduced compressibility effects. The smoother shock structure contributes to reduced drag divergence and more stable aerodynamic performance at higher Mach numbers.

The study reinforces the capability of CFD simulations in resolving complex three-dimensional aerodynamic phenomena associated with sweep. The chosen SST k-ωk model successfully captured the essential flow physics, including boundary-layer behavior, shock motion, and vortex formation, aligning with modern computational studies such as Penner et al. [2] and Ambrosino [8]. The findings highlight that sweptback wings are particularly advantageous for transonic and high-subsonic flight regimes**,** where minimizing wave drag is crucial. For lower subsonic conditions, unswept wings may still yield slightly higher lift; however, the overall aerodynamic efficiency (L/D) of the sweptback configuration remains superior for cruise performance.

Although sweep reduces wave drag, it introduces spanwise flow that may complicate stall behavior and structural design. Therefore, aerodynamic optimization should account for a trade-off between efficiency and control complexity, particularly for aircraft with high aspect ratios or flexible wings. Integration with active flow control devices or adaptive structures could mitigate these effects.

References

1. Browne, O. M. F., Simulating transonic buffet aerodynamics for transport concepts (NASA/technical conference paper), 2024. NASA Technical Reports Server
2. Penner, D. A. C., Sousa, V. C. B., Ravikumar, K., et al., Wall-modeled LES of a swept wing

ISSN: **3107-6513**

with leading-edge ice (NASA technical report / SciTech 2025). NASA Technical Reports Server
3. Mori, Y., DNS of boundary-layer transition over a transonic swept wing (AIAA conference paper), 2024. arc.aiaa.org
4. De Vincentiis, L., Transition in an infinite swept-wing boundary layer subject to surface roughness and freestream turbulence, Journal of Fluid Mechanics, 2022. Cambridge University Press & Assessment
5. Zoppini, G., Transition due to isolated roughness in a swept wing boundary layer, Physics of Fluids, 2022. AIP Publishing
6. Borodulin, *V. I.,* Roughness-induced transition delay in a swept-wing boundary layer (experimental), 2024. ScienceDirect
7. Rius-Vidales, A. F., Delay of swept-wing transition using a surface hump, Journal of Fluid Mechanics, 2025. Cambridge University Press & Assessment
8. Ambrosino, B., Stationary crossflow vortices' secondary instability: Linear and DNS comparisons, AIAA Journal, 2025. arc.aiaa.org
9. Liu, Y., Receptivity and stability analysis of stationary crossflow vortices in transonic swept wings, Aerospace (MDPI), 2023. MDPI
10. Nakagawa, K., Effects of freestream turbulence on the secondary instability in swept-wing boundary layers, 2023. ScienceDirect
11. Ghoreyshi, M., Computational study of vortex interaction characteristics for swept configurations (AIAA), 2022. arc.aiaa.org
12. Xu, X., Uncertainty quantification of aerodynamic performance for iced/swept wings, 2025.